LIQUID CRYSTALS, 2018
VOL. 45, NO. 3, 415–420
https://doi.org/10.1080/02678292.2017.1338766

Taylor & Francis
Taylor & Francis Group

Pump angle and position effects on laser emission from quasicrystal microcavity by nine-beam interference based on holographic polymer-dispersed liquid crystals

Yong Li[a], Qingguo Du[b], Zongdai Liu[a], Rui Chen[a], Haitao Dai[c] and Dan Luo[a]*

[a]Department of Electrical & Electronic Engineering, Southern University of Science and Technology, Shenzhen, China; [b]Institute of High Performance Computing, Singapore, Singapore; [c]Department of Applied Physics, College of Science, TianjinUniversity, Nankai, China

ABSTRACT

We demonstrate pump angle and position effects on lasing from all organic quasicrystal fabricated by nine-beam interference. The output wavelengths of lasing are experimentally investigated with different pump angles. The underlying mechanism is explained by the photonic band edge simulated by finite-difference time-domain method. Additionally, the position effect on lasing is also demonstrated, and the emission characteristics of lasing are studied. The mirrorless laser is featured by low cost, and simple fabrication, which enables quasicrystal based on holographic polymer-dispersed liquid crystal an all organic miniature lasing devices.

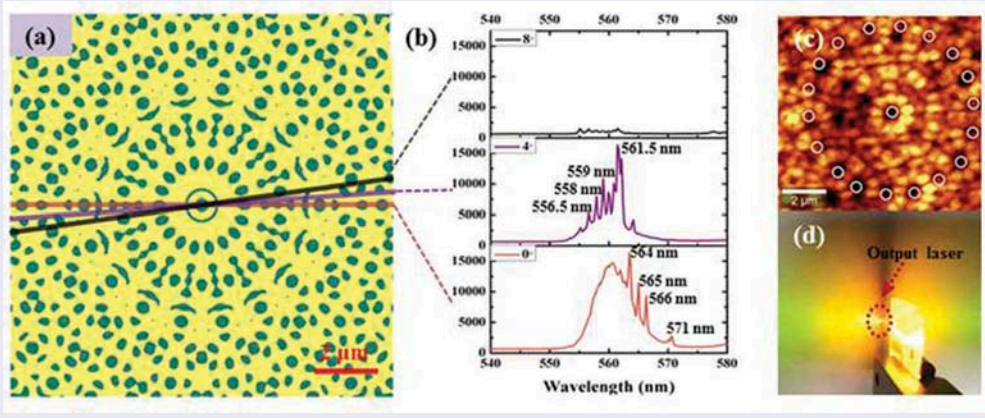

ARTICLE HISTORY
Received 28 February 2017
Accepted 1 June 2017

KEYWORDS
Dye laser; liquid crystal; microcavities; quasicrystal

1. Introduction

Organic microcavity laser based on liquid crystals (LCs) has attracted significant attention during the past decades due to its excellent tunability properties as a kind of mirrorless lasers [1]. Most of the LC lasers reported are generated due to the existence of a photonic bandgap for visible light in one-, two-, and three-dimensional periodic dielectric nanostructures, where the gain factor is significantly enhanced at the band edge [2]. LC lasers have been realised in various LC materials, such as cholesteric LC [3], ferroelectric LCs [4], blue phase LCs [5], polymer-dispersed LCs [6,7], and organic–inorganic hybrid structures [8,9]. Photonic quasicrystal, a kind of nanostructure possessing no translation symmetry but orientational symmetry, usually can be fabricated by holography lithography [10–12]. Similar to photonic crystals, the optical bandgap exists in the photonic quasicrystals [13–15]. Due to low index contrast of holographic polymer-dispersed LC (H-PDLC) [16], the position of partial optical bandgap along particular direction in photonic quasicrystal [17] plays a critical role in lasing generation, even there is no complete bandgap exist due to low index contrast.

Recently, studies on lasing for dye-doped two-dimensional H-PDLC quasicrystals have been reported. M. S. Li et al. reported multimode lasing from the microcavity of an octagonal quasicrystal [18]. In our previous study, we have investigated the lasing from Penrose quasicrystal with excellent linear polarisation and low threshold [19]. Besides external stimuli such as temperature and electric field, the microcavities of laser within the quasicrystal are highly dependent on the pump line angle as well as specific position. Different

CONTACT Dan Luo luo.d@sustc.edu.cn
*Present address: Department of Electrical & Electronic Engineering, Southern University of Science and Technology

pump condition would seriously influence the laser wavelength or even suppress the laser oscillation. However, the studies on angle and position effect on lasing from quasicrystal fabricated by nine-beam interference has never been investigated. Due to the complex structure of a quasicrystal, lasing at different wavelengths can be generated in the same device by changing the pump angle or position, which enables multiwavelength laser emission and broadens their application potential in areas such as biomedical, integrated optics, and displays.

In this paper, we demonstrate pump angle and position effects on lasing from all organic quasicrystal fabricated by nine-beam interference. The output wavelengths of lasing are experimentally investigated with different pump angles. The underlying mechanism is explained by the photonic band edge simulated by finite-difference time-domain (FDTD) method. Additionally, the position effect on lasing is also demonstrated, and the emission characteristics of lasing are studied. The mirrorless laser is featured by low cost, and simple fabrication, which enables quasicrystal based on H-PDLC an all organic miniature lasing devices.

2. Experiments

To form sample, 65 wt% monomer, trimethylolpropane triacrylate, 8 wt% cross-linking monomer, *N*-vinylpyrrollidone, 0.8 wt% photoinitiator, rose bengal, 1 wt% coinitiator, and 1.2 wt% lasing dye, PM567, all from Sigma-Aldrich (USA), and 24 wt% LC, E7 (n_o = 1.5216 and n_e = 1.7462), from Merck (Germany), were mixed together. The mixture was then filled into a cell by capillary effect, where the cell was assembled by two pieces of indium tin oxide-coated glass. The thickness of cell was 10 μm. The quasicrystal microcavity was produced through holography lithography. A prism was fabricated with side-bottom plane angle of Φ = 60° and equilateral enneagon bottom plane, indicating equal side and an equal internal angle. The material of prism was fused silica and its refractive index was 1.46. A linearly polarised Ar^+ laser (Coherent, I-306C) beam was enlarged and collimated to expose on the prism. Nine beams with wave vectors of k_n (n = 1–9) was generated and interference with each other at the bottom of prism, where the sample was adhered on. The interference pattern produced at the bottom surface of the prism was recorded by the sample cell due to the polymerisation-induced phase separation, where the polymer and LC diffuse to high- and low-intensity region, separately. The exposure intensity of each beam was ~ 9 mW/cm^2 and the exposure time

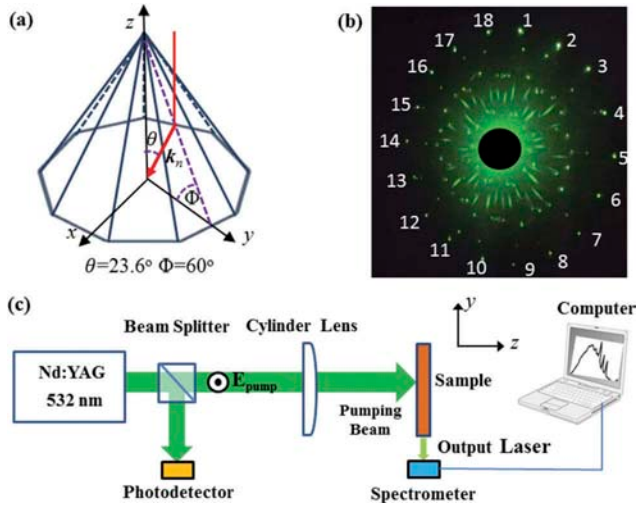

Figure 1. (Colour online) Prism used for (a) nine-beam interference. k_n is the wave vector. θ represents the angle between the beam and vertical z axis. Φ represents the side-bottom plane angle of the prism. (b) Diffraction of quasicrystal. (c) Optical setup of lasing generation.

was 120 s. The prism is shown in Figure 1(a). Here we have $\theta_1 \sim \theta_7 = \theta = 23.6°$, λ = 514.5 nm, and n_{eff} = 1.524. The diffraction image of the fabricated quasicrystal with 18 diffraction points, which is generated by a He–Ne laser with wavelength of 543 nm, is demonstrated in Figure 1(b), confirming the existence of N-fold quasicrystals $2N$ diffraction points. For the lasing generation, a Q-switched frequency-doubled Nd:yttrium-aluminium-garnet pulsed laser (Quantel, Q-smart 450) was focused by a cylinder lens (Thorlabs, LJ1629L1-A, f = 150 mm) and incident on the surface of the sample in a shape of narrow line (width: ~0.5 nm), as shown in Figure 1(c). The wavelength, pulse duration, and repetition of pump laser was 532 nm, 10 ns, and 10 Hz, respectively. The pump laser was linearly polarised. A beam splitter and photodetector were used to measure the pump energy. The output laser was received by a computer-connected spectrometer (USB2000+, Ocean optics, resolution of 0.05 nm).

3. Results and discussion

The lasing from our quasicrystal was also studied in different directions at a pumping power level of 0.050 mJ/pulse (Figure 2). Figure 2(a) shows the simulated binary pattern of quasicrystal. The pump directions of 0°, 4°, and 8° are marked by red, purple, and black, respectively. It can be seen that a lasing blue shift was observed while the direction was changed from angle 0° to 4° with respect to the x axis, where the main peaks shifted from 564/565/566/571 nm to 555/556.5/558/559/560/561/561.5/562/564 nm, as shown

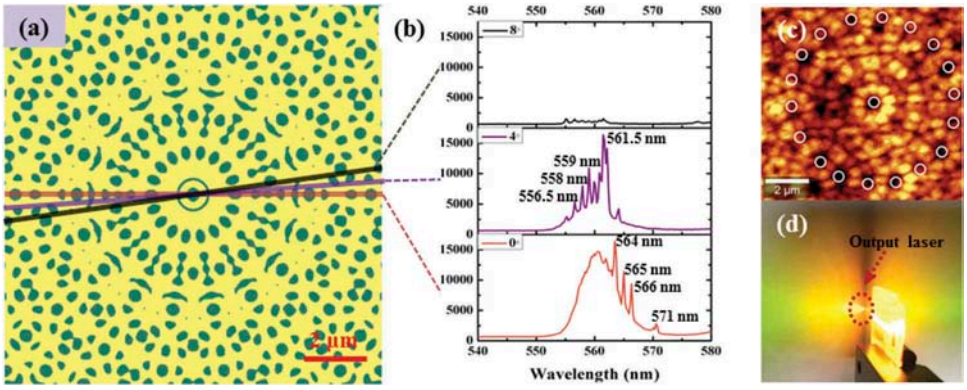

Figure 2. (Colour online) (a) Schematic of the lasing generated along different angles of nine-beam quasicrystal. Three different angles: 0°, 4°, and 8° are used. The scale bar is 2 μm. (b) Spectra obtained at tilt angles of 0°, 4°, and 8°, respectively. The wavelength of lasing blue shifts from 0° to 4°, and disappears at 8°. (c) Image measured by AFM. The scale bar is 2 μm. (d) Image of output laser.

in Figure 2(b). The laser oscillation blue shifts to the shorter wavelength range. At the angle of 8°, the lasing oscillation was largely suppressed and no significant laser peaks were observed. We can see that the different lasing modes have their preferred lasing directions and a reverse lasing blue shift was observed while the direction was changed from angle 8° to 0° with respect to the x axis. It is noted that since the quasicrystal formed by nine-beam interference possesses the rotational symmetry, with a rotational angle of 20° (360°/2N, N = 9), the experienced structure is actually the same for light oscillating at the direction pairs of 0°/20°, 4°/16°, and 8°/12°, respectively. Figure 2(c) shows the atomic force microscopy (AFM) image of quasicrystal, indicating the experimental result is consistent with the simulation. The image of laser is shown in Figure 2(d), where the divergence of laser beam is around 8.25°.

The photoluminescence spectral of laser dye PM567, with peak emission wavelength ~580 nm, and the calculated transmittance spectra that is simulated by a commercial FDTD software package Lumerical both are shown in Figure 3. The red, purple, and black curves represent the transmittance along the tilt angles of 0°, 4°, and 8°, respectively. The photonic band edges are represented by corresponding colours, and the positions of lasing peaks are marked by rectangle box. For 0° and 4° cases, these wavelengths are located at the photonic band edge, which corresponds to the half way of the transmittance maxima and minima. These positions are preferable for laser action because of the field enhancement of stimulated emission [17]. The lasing from the quasicrystal should be related to the reduced group velocity that leads to large and increased density of states. In contrast, for 8° case, the photoluminescence of laser dye is overlapped with a range that is not the photonic band edge. It

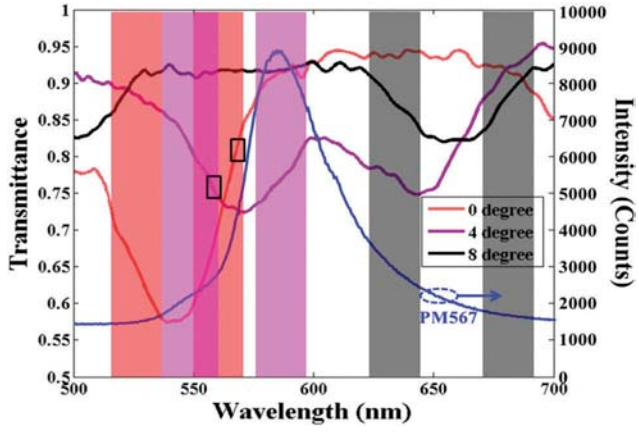

Figure 3. (Colour online) Simulated transmittance of quasicrystal formed by nine-beam interference along different tilt angles, where the photonic band edges are represented by corresponding colours. The photoluminescence of PM567 is also shown.

can be seen that the transmittance is relatively flat in the range of 550–565 nm, which results in a non-reduced group velocity, and thus a small density of states. Therefore, there was no lasing generation. We can see that the simulated results are consistent with the experimental results. The mechanism of laser generation along different angles can be explained well. Based on the simulated transmittance, and the band edge of transmittance, we can control the laser wavelength. For example, for tilt angle of 0°, the expected laser emissions should be in the range of 510–580 nm. In contrary, the laser should occur in the range of 620–690 nm or less than 530 nm. It can be realised by doping different kinds of laser dyes. When the pump energy reaches 0.266 mJ/pulse, the laser dye will be blanched that leads to reduced output lasing energy.

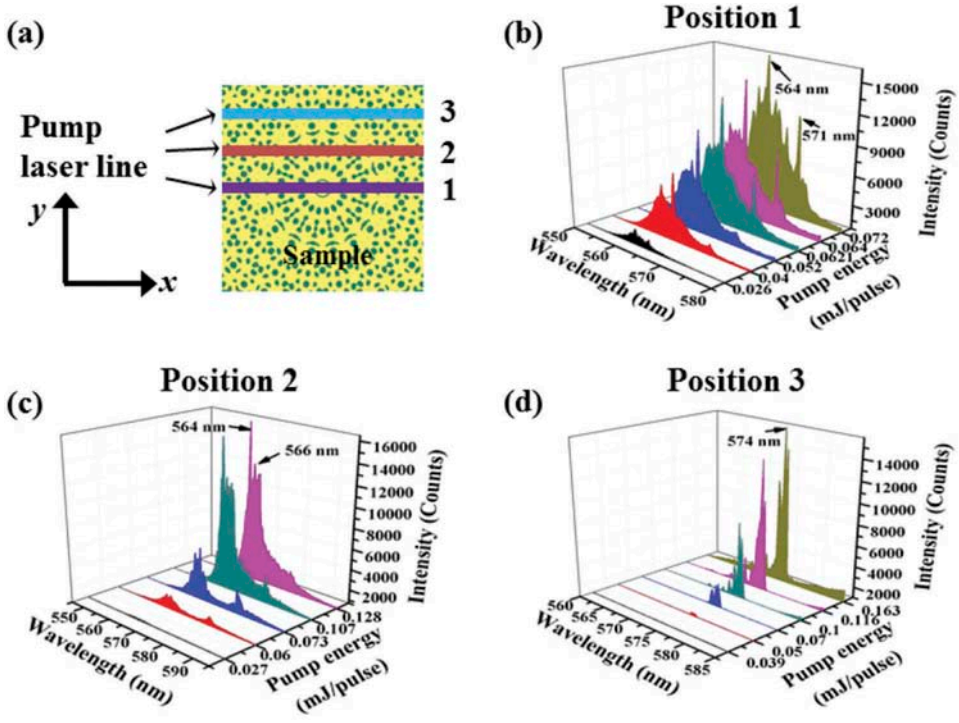

Figure 4. (Colour online) (a) Schematic of the lasing generated along different lines of nine-beam quasicrystal. Spectrum of lasing from quasicrystal formed by nine-beam interference measured along (b) line 1, (c) line 2, and (c) line 3.

In our experiment, the lasing was also generated at several different positions along x axis. The corresponding pump lines and obtained lasing spectral are shown in Figure 4(a–d), respectively. In Figure 4(a), those lines are parallel to each other and separated by around 1 mm, where line 1 crosses to the centre of the quasicrystal and is along x axis and lines 2 and 3 are parallel to line 1 but far from the centre of the

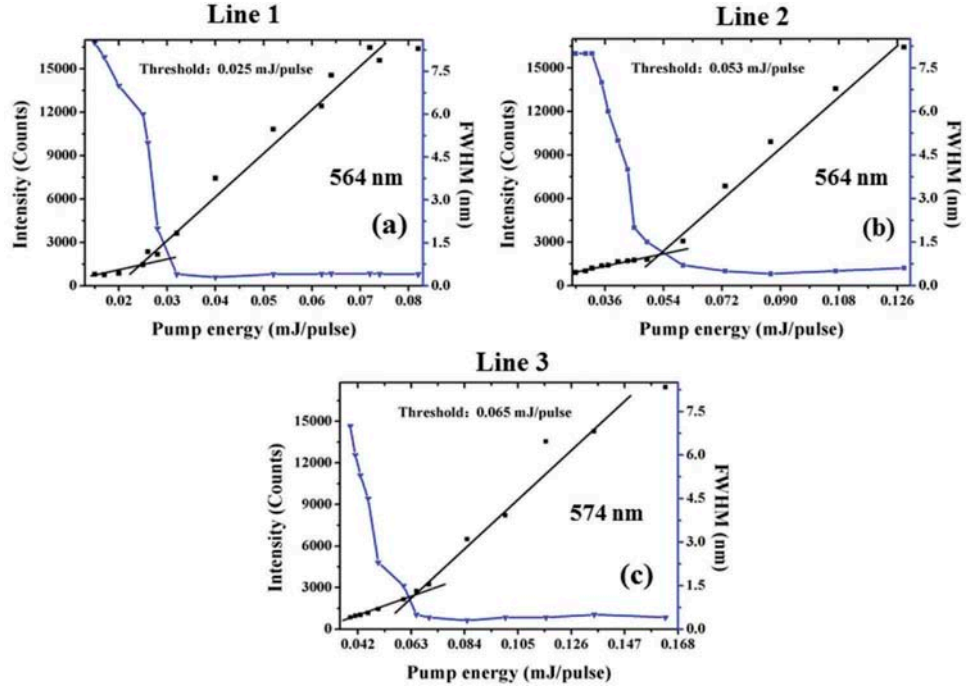

Figure 5. (Colour online) The intensity and line width versus pumping energy: (a) 564 nm, (b) 564 nm, and (c) 574 nm for nine-beam formed quasicrystal along lines 1–3.

quasicrystal. Figure 4(b–d) shows the lasing spectra measured at different positions (along lines 1–3) under different pump energies for nine-beam quasicrystal, respectively. The lasing peaks of 564 & 571 nm, 564 & 566 nm, and 574 nm were observed and depicted on the profile of the lasing spectrum with an increase of pump energy up to 0.072, 0.128, and 0.163 mJ/pulse. The lasing peak varied with the pump line positions, which indicated that the output lasing was determined by both local structures of quasicrystal the pump light experienced and the photoluminance of doped laser dye. Therefore, the wavelength of output lasing peak was determined by local pump position and laser dye doped. The local structures of different parallel pump lines were quite different from each other due to the lack of translation symmetry in quasicrystal in our experiment. If the pump line was further shifted away from the centre of the quasicrystal, the wavelength of laser peak exhibited a random trend, which was not necessarily a red shift as we demonstrated in Figure 4(b–d).

The lasing intensity and line width at lasing peaks versus pump energy at different pump lines for nine-beam interference quasicrystal are shown in Figure 5 (a–c). The lasing thresholds are 0.025, 0.053, and 0.065 mJ/pulse at 564, 564, and 574 nm, corresponding to lines 1–3. In all cases, the line width of lasing peaks narrows with the increase of pump energy. The line widths all reduce to less than 1 nm when the pump energies are beyond the thresholds.

4. Conclusion

In conclusion, the pump angle and position effects on lasing from all organic quasicrystal fabricated by nine-beam interference have been demonstrated. The output lasing wavelengths at different pump angles are measured experimentally. With increase of angle from 0° to 8°, lasing peaks firstly blue shift and then disappear. The angle dependent property could be understood by photonic band edge in transmittance which is simulated by the FDTD method. The simulation result is highly consistent with the experimental result. Additionally, the position effect on lasing is also demonstrated, and the emission characteristics of lasing are studied.

Acknowledgement

This work is supported by Natural National Science Foundation of China (NSFC) (61405088); Shenzhen Science and Technology Innovation Council (JCYJ20160226192528793, JCYJ20150930160634263, and KQTD2015071710313656).

Disclosure statement

No potential conflict of interest was reported by the authors.

Funding

This work was supported by Natural National Science Foundation of China (NSFC) [61405088]; Shenzhen Science and Technology Innovation Council [JCYJ20160226192528793, JCYJ20150930160634263, and KQTD2015071710313656].

References

[1] Coles H, Morris S. Liquid-crystal lasers. Nat Photon. 2010;4:676–685.
[2] Dowling JP, Scalora M, Bloemer MJ, et al. The photonic band edge laser: a new approach to gain enhancement. J Appl Phys. 1994;75:1896–1899.
[3] Kopp VI, Fan B, Vithana HK, et al. Low-threshold lasing at the edge of a photonic stop band in cholesteric liquid crystals. Opt Lett. 1998;23:1707–1709.
[4] Ozaki M, Kasano M, Ganzke D, et al. Mirrorless lasing in a dye-doped ferroelectric liquid crystal. Adv Mater. 2002;14:306–309.
[5] Cao W, Muñoz A, Palffy-Muhoray P, et al. Lasing in a three-dimensional photonic crystal of the liquid crystal blue phase II. Nat Mater. 2002;1:111–113.
[6] Liu YJ, Sun XW, Shum P, et al. Low-threshold and narrow-linewidth lasing from dye-doped holographic polymer-dispersed liquid crystal transmission gratings. Appl Phys Lett. 2006;88:061107.
[7] Luo D, Sun XW, Dai HT, et al. Two-directional lasing from a dye-doped two-dimensional hexagonal photonic crystal made of holographic polymer-dispersed liquid crystals. Appl Phys Lett. 2009;95:151115.
[8] Wang H–T, Lin J-D, Lee C-R, et al. Ultralow-threshold single-mode lasing based on a one-dimensional asymmetric photonic bandgap structure with liquid crystal as a defect layer. Opt Lett. 2014;39:3516–3519.
[9] Huang J-C, Hsiao Y-C, Lin Y-T, et al. Electrically switchable organo-ingorganic hybrid for a white-light laser source. Sci Rep. 2016;6:28363.
[10] Shechtman D, Blech I, Gratias D, et al. Metallic phase with long-range orientational order and no translational symmetry. Phys Rev Lett. 1984;53:1951–1953.
[11] Rotenberg E, Theis W, Horn K, et al. Quasicrystalline valence bands in decagonal AlNiCo. Nature. 2000;406:602–605.
[12] Gorkhali SP, Qi J, Crawford GP. Switchable quasi-crystal structures with five-, seven-, and ninefold symmetries. J Opt Soc Am B. 2006;23:149–158.
[13] Chan YS, Chan CT, Liu ZY. Photonic band gaps in two dimensional photonic quasicrystals. Phys Rev Lett. 1998;80:956–959.
[14] Zoorob ME, Charlton MDB, Parker GJ, et al. Complete photonic bandgaps in 12-fold symmetric quasicrystals. Nature. 2000;404:740–743.
[15] Man W, Megens M, Steinhardt PJ, et al. Experimental measurement of the photonic properties of icosahedral quasicrystals. Nature. 2005;436:993–996.

[16] Bunning TJ, Natarajan LV, Tondiglia VP, et al. Holographic polymer-dispersed liquid crystals (H-PDLCs). Annu Rev Mater Sci. 2000;30:83–115.
[17] Sutherland RL, Tondiglia VP, Natarajan LV, et al. Switchable orthorhombic F photonic crystals formed by holographic polymerization-induced phase separation of liquid crystal. Opt Express. 2002;10:1074–1082.
[18] Li MS, Fuh AY, Wu ST. Multimode lasing from the microcavity of an octagonal quasi-crystal based on holographic polymer-dispersed liquid crytals. Opt Lett. 2012;37:3249–3251.
[19] Luo D, Du QG, Dai HT, et al. Strongly linearly polarized low threshold lasing of all organic photonic quasicrystals. Sci Rep. 2012;2:627.